

A New Coupled Model for Alloy Solidification

Daming Li, Ruo Li and Pingwen Zhang *

February 6, 2004

Abstract

A new coupled model in the binary alloy solidification has been developed. The model is based on the cellular automaton(CA) technique to calculate the evolution of interface governed by temperature, solute diffusion and Gibbs-Thomson effect. The diffusion equation of temperature with the release of latent heat on the solid/liquid (S/L) interface is valid in the entire domain. The temperature diffusion without the release of latent heat and solute diffusion are solved in the entire domain. In the interface cells, the energy and solute conservation, thermodynamic and chemical potential equilibrium are adopted to calculate the temperature, solid concentration, liquid concentration and the increment of solid fraction. Comparing with other models where the release of latent heat is solved in implicit or explicit form according to the solid/liquid(S/L) interface velocity([21], [23]), the energy diffusion and the release of latent heat in this model are solved at different scales, i.e., the macro-scale and micro-scale. The variation of solid fraction in this model is solved using several algebraic relations coming from the chemical potential equilibrium and thermodynamic equilibrium which can be cheaply solved instead of the calculation of S/L interface velocity. With the assumption of the solute conservation and energy conservation, the solid fraction can be directly obtained according to the thermodynamic data. This model is natural to be applied to multiple(> 2) spatial dimension case and multiple(> 2) component alloy. The morphologies of equiaxed dendrite are obtained in numerical experiments.

Keywords: Alloy solidification, Dendritic growth, Cellular automaton, Segregation.

1 Introduction

During the last two decades, many numerical models have been developed to understand the evolution of dendrite's growth in solidification of alloys as an alternative approach from experimental techniques([1], [2]) and analytical models([3]-[7]). Those numerical models developed for simulating microstructure evolution in solidification of alloys are classified into two groups: deterministic and stochastic models. Phase field models(PFM)([8]-[13]) have been known as one of the most adequate deterministic models for directly simulating the dendrite's growth. Other valuable tracking methods of S/L interface, that can be used for simulating dendrite's growth, are described in details in [14] and [15]. Stochastic method such as the Monte Carlo method or the cellular automaton have been applied to the prediction of macrostructure grain structure. The Monte Carlo method ([16], [17]) has been used to predict the solid-state transformation such as crystallization or grain structure, whilst

*LMAM, CCSE & School of Mathematical Sciences, Peking University, E-mail: lidaming@pku.edu.cn, rli@math.pku.edu.cn, pzhang@math.pku.edu.cn

the cellular automaton model that account for the dendrite's growth kinetics has been applied to simulate the solidification grain structures and the columnar to equiaxed transition.

The main idea of cellular automaton model is as follows. The whole domain is triangulated into cells. All the cells are divided into three class: solid cells, liquid cells and interface cells corresponding to solid fraction 1, 0 and in the open interval $(0, 1)$. The governing equations of temperature and solute concentration are solved in the whole domain. The S/L interface is assumed to be located in the interface cells. The solid fraction in the interface cells are updated whenever the temperature and solute concentration there are changed. When the solid fraction in the interface cells is updated to 1, it is set to be solid cells. The new solidified cells will capture some neighboring liquid cells according to certain rules and set them as interface cells. It is then clear the cellular automaton model have three parts in the whole algorithm: (i) solving the governing equations of temperature and solute concentration; (ii) updating the solid fraction in the interface cells; (iii) capturing the liquid cells neighboring the new solidified cells as interface cells.

Brown *et al* [18] and Sasikumar *et al* [19] tried to simulate thermal dendrites using the cellular automaton. The effect of thermal diffusion, undercooling and surface tension etc, on the morphology of thermal dendrites, are researched.

Dilthy *et al* [20] developed models for thermal and solutal dendrites. Their simulated results were visually compared with experimental microstructure obtained in welding with remarkable agreement. Their models included a methodology to reduce the artificial anisotropy of the CA mesh. The model for solutal dendrites does not incorporate the solution of heat equation. Consequently, a temperature gradient was imposed to simulate constrained growth.

Nastac [21] developed a model for solutal dendrite that is able to reproduce the same qualitative features as previous model. Moreover, it solves the heat equation enabling the simulation of constrained and unconstrained growth. The model can simulate the columnar-to-equiaxed transition, showing the complex interactions between growth dendrites in the same melt.

Jacot *et al* [22] proposed a pseudo-front tracking technique for the modelling of solidification micro-structures in multi-component alloys. Cell capture like CA model is also used, but the S/L interface in interface cells was explicitly tracked to calculate the curvature undercooling according to solid fraction. Solid fraction in the interface cells was calculated by level rule method instead of the calculation of the S/L interface velocity. Moreover, hexagonal mesh was used to reduce artificial anisotropy. The agreement was shown by comparing their model with PFM, but their results are based on the assumption of uniform temperature on the scale of calculated domain.

Beltran-Sanchez *et al* [23] reconsidered the quantitative capability of CA model and simulated the columnar-to-equiaxed transition, showing the complex interactions between dendrites. Moreover, mesh independency was obtained if the curvature was calculated in a local meaning, instead of empirical formula, such as cell counting proposed by Nastac [21], etc. But their model is limited only to the simulation of dendrites in binary alloys systems.

All those works assumed there is a clear S/L interface in the domain under consideration. Certain evolution mechanism of this S/L interface should be adopted. The updating of the solid fraction in the interface cells is then calculated according to the S/L interface. The assumption of a clear S/L interface requires some cell resolution operations either explicitly or implicitly.

In this paper, a new coupled model for the simulation of crystal growth in alloy systems based on cellular automaton model has been developed. The solution methodology is performed at two scales level. At the macro-scale level, the temperature diffusion without the release of latent heat and solute

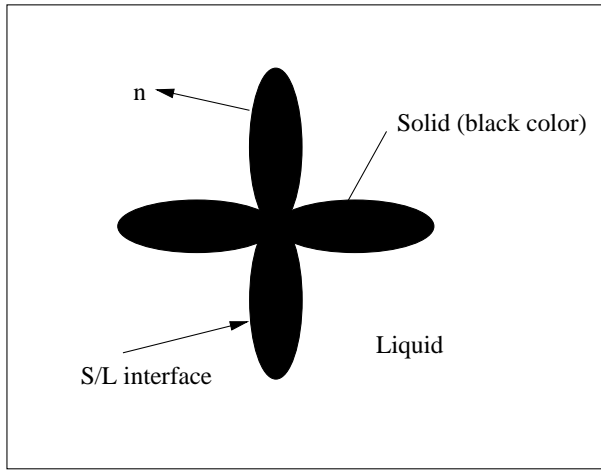


Figure 1: Schematic representation of solidification domain Ω .

diffusion are solved in the entire domain using general numerical scheme for parabolic systems. At the micro-scale level, the temperature, solid concentration, liquid concentration and the increment of solid fraction are solved by solving the algebraic equations from the energy and solute conservation, chemical potential equilibrium and thermodynamic on the S/L interface. Different from other models where the release of latent heat is solved in implicit or explicit forms, the energy diffusion and the release of latent heat in our model are solved at different scales, i.e., the macro scale and micro scale. Moreover, the increment of solid fraction in this model is very easy to solve, instead of calculating the S/L interface velocity ([21], [23]). It is trivial to extend this model to any multi-component alloy system and to apply directly to any spatial dimensional case if the thermodynamic data are known.

The paper is organized as follows. The mathematical description of the model is presented in Section 2. The numerical scheme is described in Section 3. In Section 4, both two dimensional and three dimensional equiaxed dendrite are showed. Conclusions are presented in Section 5.

2 Governing Equation of the Solidification Process of Binary Alloys

To describe the dendrite's solidification process in a binary alloy on a given rectangle domain Ω (see the model in a restricted two dimensional domain in Figure (1)), the following physical quantities should be resolved during the process: the temperature T , the solid solute concentration C_S , the liquid solute concentration C_L and the solid fraction f_S , which tells how much part of the alloy is solidified.

The equations that describes the physics of the solidification process then are as follows. Temperature T in Ω (heat diffusion equation)

$$\rho c_p \frac{\partial T}{\partial t} = K \Delta T + \rho L \frac{\partial f_S}{\partial t}, \quad \text{in } \Omega \quad (2.1)$$

where t is time, ρ is the density, c_p is the specific heat, K is the thermal conductivity, L is the latent heat of solidification. For simplicity, we denote the liquid fraction as $f_L := 1 - f_S$. The following boundary condition at the walls of the domain is adopted:

$$-K \nabla T \cdot \mathbf{n} = h(T - T_\infty) \quad (2.2)$$

where \mathbf{n} is the unit out normal to the wall, h is the coefficient of heat transfer by conduction, and T_∞ is the environment temperature. Concentration (C) in Ω (solute diffusion equation):

$$\frac{\partial C_L}{\partial t} = \nabla(D_L \nabla C_L), \quad \text{in the liquid phase} \quad (2.3)$$

$$\frac{\partial C_S}{\partial t} = \nabla(D_S \nabla C_S), \quad \text{in the solid phase} \quad (2.4)$$

where D_L and D_S are the liquid and solid diffusion coefficient, respectively. Zero flux boundary conditions are applied at the four walls of the simulation domain Ω .

Above equations are not closed because there should be boundary conditions between the liquid phase and solid phase for the solute diffusion equation. The diffusion equations for the solute concentration in the liquid phase and solid phase can be combined together to obtain the governing equation for solute $C = f_S C_S + f_L C_L$ as

$$\frac{\partial C}{\partial t} = \nabla(f_L D_L \nabla C_L) + \nabla(f_S D_S \nabla C_S), \quad \text{in } \Omega \quad (2.5)$$

which is valid on the whole domain. The derivation of (2.5) can be found in [26].

On the S/L interface, the physics of the solidification process can be described by chemical potential equilibrium and the thermodynamic equilibrium. If the discrepancy from the equilibrium solidification is not so dramatic, the chemical potential equilibrium gives a linear relationship of the liquid solute concentration and solid solute concentration

$$C_S^* = k C_L^* \quad (2.6)$$

where k is the equilibrium partition coefficient. The superscript $*$ means at the S/L interface.

Assume local thermodynamic equilibrium at the interface, the interface temperature T^* and liquid solute concentration satisfies

$$T^* = T_L^{EQ} + (C_L^* - C_0)m_L - \Gamma \kappa f(\varphi, \theta) \quad (2.7)$$

where C_0 is the initial concentration, T_L^{EQ} is the equilibrium liquidus temperature at the initial composition, m_L is the slope of the liquidus, Γ is the Gibbs-Thomson coefficient, κ is the curvature of S/L interface, θ is the angle of the preferential growth direction with respect to a referential axis, φ is the angle of the normal to the interface with respect to the same axis, and the anisotropy of the surface tension is described by function $f(\varphi, \theta)$, which is proposed by [23]:

$$\begin{aligned} f(\varphi, \theta) = & (1/3.19)(-0.117 \cos(4(\varphi - \theta)) \\ & - 0.163 \cos(8(\varphi - \theta)) \\ & - 0.0358 \cos(16(\varphi - \theta)) + 3.19) \end{aligned}$$

where

$$\varphi = \cos^{-1} \left(\frac{\partial f_S / \partial x}{\sqrt{(\partial f_S / \partial x)^2 + (\partial f_S / \partial y)^2}} \right). \quad (2.8)$$

For the growth of four-fold symmetry of the cubic crystal, θ takes from $-\pi/4$ to $\pi/4$. (2.7) is in fact the linear approximation of the thermodynamic data. The interface temperature T^* is also affected by the S/L interface velocity, which can be omitted at very low solidification velocity.

3 The Model and Numerical Schemes

A basic difference of our model from others is the release of latent heat is not involved in governing equation of the temperature. The computation domain Ω is triangulated into square cells of dimensions small enough to resolve the dendrite features of interest. The detailed description of CA technique can be found in [20] and [21]. The geometry of the cells is square. Each cell has three possible states: liquid, interface or solid. The preferential growth direction is aligned with the direction of cells, i.e., $\theta = 0$ or $\pi/4$, neighbor capture rule as in [23] is adopted.

3.1 Temperature and Solute Diffusion - Macro-scale Level

Let us introduce some finite difference notations at first for simplicity

$$\begin{aligned}
D_x u_{i,j} &:= \frac{u_{i+1/2,j} - u_{i-1/2,j}}{\Delta x} \\
D_y u_{i,j} &:= \frac{u_{i,j+1/2} - u_{i,j-1/2}}{\Delta y} \\
D_x^2 u_{i,j} &:= \frac{u_{i+1,j} - 2u_{i,j} + u_{i-1,j}}{\Delta x^2} \\
D_y^2 u_{i,j} &:= \frac{u_{i,j+1} - 2u_{i,j} + u_{i,j-1}}{\Delta y^2} \\
\Delta_h u_{i,j} &:= D_x^2 u_{i,j} + D_y^2 u_{i,j}
\end{aligned} \tag{3.9}$$

The temperature diffusion equation (2.1) without the release of latent heat $\rho L \frac{\partial f_s}{\partial t}$ is solved using backward Euler scheme in temporal direction and central finite difference scheme in spatial direction as

$$\frac{T_{i,j}^{(n+1)} - T_{i,j}^{(n)}}{\Delta t} = K \Delta_h T_{i,j}^{(n+1)} \tag{3.10}$$

where Δt is the time step size and Δx , Δy are the spatial step size in x and y direction. In our computation, Δx and Δy are equal. The resulted linear algebraic system is solved with an algebraic multigrid solver(AMG). The latent heat is calculated in the micro-scale level in next subsection.

The solute diffusion equation is discretized directly with forward Euler scheme in temporal direction and central difference scheme in the spatial direction. Explicit scheme is adopted, different from the scheme of the temperature diffusion equation, because the diffusion coefficient for the solute is much smaller than that of the heat. The quantity crossing the interface cells are calculated with simple algebraic average. The discretized equation is then as

$$\begin{aligned}
\frac{C_{i,j}^{(n+1)} - C_{i,j}^{(n)}}{\Delta t} &= D_x (F_{S;i,j} + F_{L;i,j}) + D_y (G_{S;i,j} + G_{L;i,j}) \\
F_{S;i,j} &= D_S \frac{f_{S;i-1/2,j} + f_{S;i+1/2,j}}{2} D_x C_{S;i,j}^{(n)} \\
F_{L;i,j} &= D_L \frac{f_{L;i-1/2,j} + f_{L;i+1/2,j}}{2} D_x C_{L;i,j}^{(n)} \\
G_{S;i,j} &= D_S \frac{f_{S;i,j-1/2} + f_{S;i,j+1/2}}{2} D_y C_{S;i,j}^{(n)} \\
G_{L;i,j} &= D_L \frac{f_{L;i,j-1/2} + f_{L;i,j+1/2}}{2} D_y C_{L;i,j}^{(n)}
\end{aligned} \tag{3.11}$$

3.2 Chemical Potential and Thermodynamic Equilibrium - Micro-scale Level

After the calculation of the temperature T and concentration C at the macro-scale level, the temperature, solid concentration, liquid concentration and the solid fraction should be adjusted to satisfy chemical potential equilibrium (2.6) and thermodynamic equilibrium (2.7). The philosophy in this model is: if the energy, the solute and curvature undercooling at an interface cell is given, the solid fraction in this cell must be known according to the thermodynamic data. After a numerical stepping forward (3.10) and (3.11), the total energy, including the heat and latent energy, in a given interface cell (i, j) is $c_p T_{i,j} - L f_{S;i,j}$ and the total solute in this cell is $C_{i,j}$. But the set of quantities $f_{S;i,j}$, $T_{i,j}$, $C_{S;i,j}$ and $C_{L;i,j}$ in this cell do NOT satisfied the chemical potential equilibrium and thermodynamic equilibrium at the S/L interface. This set of quantities is then updated to $f'_{S;i,j}$, $T'_{i,j}$, $C'_{S;i,j}$ and $C'_{L;i,j}$ to satisfy the chemical potential equilibrium and thermodynamic equilibrium. We will omit the location subscript i,j in this subsection since the operation is constrained on the data in this interface cell. Considering the conservations and equilibriums listed above, we have the following algebraic system:

$$\begin{aligned}
 T' &= T + \frac{L}{c_p}(f'_S - f_S) \\
 C &= f'_S C'_S + (1 - f'_S) C'_L \\
 T' &= T_L^{EQ} + (C'_L - C_0) m_L + \Gamma \kappa f(\varphi, \theta) \\
 C'_S &= k C'_L
 \end{aligned} \tag{3.12}$$

where we assume that the concentrations on the scale of the interface cells are uniform [22], i.e.,

$$C_S = C'_S = k C'_L = k C_L \tag{3.13}$$

is valid in the interface cells. The curvature cooling $\Gamma \kappa f(\varphi, \theta)$ is calculated from the data at previous time step. Solving the four algebraic equations (3.12), let us show the four unknowns, i.e., the temperature T' , solid concentration C'_S , liquid concentration C'_L and the solid fraction f'_S are uniquely determined. Eliminating T' , C'_S and C'_L , we get the equation of f'_S :

$$\frac{L}{c_p} (f'_S)^2 - \left(A + \frac{L}{c_p(1-k)} \right) f'_S + \frac{A + C m_L}{1-k} = 0. \tag{3.14}$$

where

$$A = T_L^{EQ} - C_0 m_L - T - \Gamma \kappa f(\varphi, \theta) + \frac{L}{c_p} f_S. \tag{3.15}$$

It is easy to show that in the two roots of (3.14), there are only one $f'_S \in [f_S, 1]$ if $T_a \leq T \leq T_c$, and $f'_S \in [0, f_S]$ if $T_c \leq T \leq T_b$, where

$$\begin{aligned}
 T_a &= T_S(C) - \frac{L}{c_p}(1 - f_S) \\
 T_b &= T_L(C) + \frac{L}{c_p} f_S \\
 T_c &= T_L^{EQ} - C_0 m_L + \frac{C m_L}{1 - (1-k) f_S} \\
 T_S(C) &= T_L^{EQ} + \left(\frac{C}{k} - C_0 \right) m_L \\
 T_L(C) &= T_L^{EQ} + (C - C_0) m_L
 \end{aligned} \tag{3.16}$$

$T_S(C)$ and $T_L(C)$ are the solidus and liquidus temperature at the concentration C , respectively.

L (J/Kg)	ρ (J/m ³)	K (W/m K)
2.70×10^5	7300	30
c_p (J/Kg K)	$T_L^{E/Q}$ (°C)	Γ (K m)
800	1490	1.9×10^{-7}
k(-)		0.34
D_L (m ² /s)		2.0×10^{-9}
D_S (m ² /s)		5.0×10^{-10}
m_L (°C/%)		-80

Table 1: Thermophysical properties for Fe-0.6wt%C used in simulation

At the same time, the interface cell will become solid cell ($f'_S \geq 1$) if $T \leq T_a$, or liquid cell ($f'_S \leq 0$) if $T \geq T_b$. In order to show how to choose the suitable root if there are two roots in equation (3.14), we eliminate T' , C'_S and f'_S to get the equation of C'_L

$$m_L(C'_L)^2 + \left(A - \frac{L}{c_p(1-k)} \right) C'_L + \frac{L}{c_p} \frac{C}{1-k} = 0. \quad (3.17)$$

It can be verified there is only one root of equation (3.17) in $[C, C/k]$ if $T_a \leq T \leq T_b$. Once C'_L is known, the other three unknowns can be obtained from (3.12). The calculation of the increment of solid fraction in (3.12) is different with other model, where the temperature of the interface cells is known from the previous time, leading to the thermodynamic equilibrium (2.7) is not satisfied simultaneously ([19], [23]). Moreover, we need not calculate the velocity of the S/L interface as [21] and [23] for calculating the concentration distribution in the interface cell.

3.3 Calculation of time-step and curvature

The time-step Δt is calculated from

$$\Delta t = \eta \min\left(\frac{\Delta x}{V_{\max}}, \frac{\Delta x^2}{D_L}, \frac{\Delta x^2}{D_S}\right) \quad (3.18)$$

where η is a constant less than 1, which should be choose suitably in our simulation and Δf_S is the increase of solid fraction in one time-step and the Δt at the right hand side is for the last time step.

The calculation of curvature, mentioned by Nastac [21], and originally proposed by Kothe *et al* [24], relies on the computation of the local curvature,

$$\begin{aligned} \kappa &= -(\nabla \cdot \mathbf{n}) \\ &= \frac{1}{|\vec{n}|} \left[\left(\frac{\vec{n}}{|\vec{n}|} \cdot \nabla \right) |\vec{n}| - (\nabla \cdot \vec{n}) \right] \\ &= \frac{2(f_S)_x(f_S)_y(f_S)_{xy} - (f_S)_y^2(f_S)_{xx} - (f_S)_x^2(f_S)_{yy}}{[(f_S)_x^2 + (f_S)_y^2]^{3/2}} \end{aligned} \quad (3.19)$$

where the unit normal $\mathbf{n} = \vec{n}/|\vec{n}|$ and normal vector $\vec{n} = \nabla f_S$.

3.4 Algorithm

The cell capture in our computation is the same as in [21]. Further result on capturing rules will be reported in the future. Omitting the nucleation of dendrites of selected crystallographic orientation at the initial stage, the whole algorithm is as:

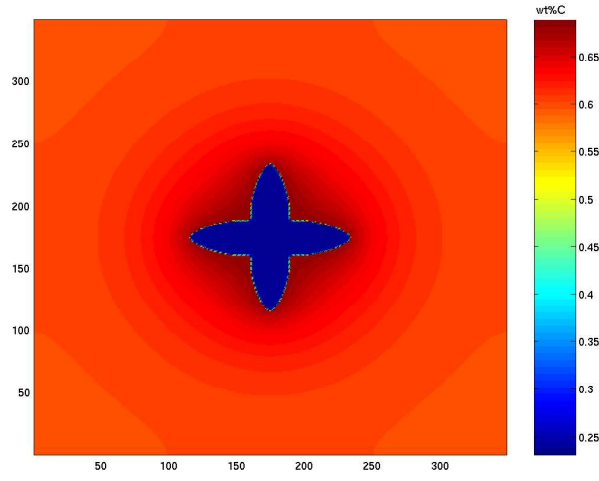


Figure 2: solute concentration at solidification time 0.2s

- Step 1: Initialization.
- Step 2: Calculation of time-step.
- Step 3: Calculation of solutal field C .
- Step 4: Calculation of temperature T without the release of latent heat.
- Step 5: Calculation of solid fraction in the interface cells.
- Step 6: Restore C_L, C_S for all cells. For the solid or liquid cells, it is obvious how to define C_L, C_S . For the interface cells, after the change of solid fraction, the solute rejection or absorption is calculated so as to maintain solute balance in the interface cells.
- Step 7: Cell capture. Return to Step 2.

4 Numerical Experiments

The binary alloy Fe-0.6wt%C is used in the simulation. The initial temperature and concentration are $T_L^{EQ} = 1490^\circ C$, $C_0 = 0.6\text{wt}\%$ for component C, respectively. The environment temperature T_∞ is 298 K. Other thermophysical properties used in our simulation is listed in Table 1. The square mesh $n \times n$ is generated from the square domain Ω .

4.1 Growth of one equiaxed dendrite

To simulate the growth of one equiaxed dendrite, the following conditions as [23] was performed. The wall of simulated domain Ω with the size of $10^{-4}m$ was cooled under a constant heat transfer coefficient $h = 10 \text{ W/m}^{-2} \text{ K}^{-1}$. A single grain was nucleated at the center of the domain, with the composition kC_0 . Because the calculation of temperature is decoupled by macro-micro process, which lead to the need of small time-step to obtain stable results, we choose $\eta = 0.025$ and $n = 350$, i.e.

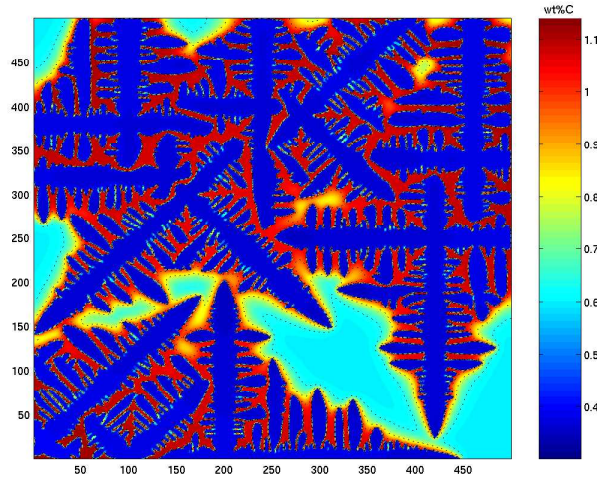


Figure 3: solute concentration at solidification time 0.6s

$\Delta x = 2.8571 \times 10^{-4} \text{m}$ and $\Delta t = 1.0204 \times 10^{-6} \text{s}$. The simulation result was shown in Figure 2, where the solidification time is 0.2 seconds. The dendrite's morphology in our result is same as those in [23]. Moreover, the dendrite morphology changes very small if the time step size and spatial step size is reduced.

4.2 Interaction of multiple equiaxed dendrites

Our model was used to simulate the solidification structure of multiple equiaxed dendrites. The same conditions as [23] was used. The size of simulated domain is $250 \mu\text{m}$ and cell size is $0.5 \mu\text{m}$ and $\eta = 0.0625 (\Delta t = 7.8125 \times 10^{-6} \text{s})$. The coefficient of heat transfer coefficient $h = 1000 \text{ W/m}^{-2} \text{ K}^{-1}$. The nucleation location of ten grains with crystallographic directions 0° and 45° is almost same as the conditions in [23]. The neighbor capture rule for grains with crystallographic directions 0° and 45° was used [23]. The interaction of multiple grains with different preferential crystallographic orientation was shown with different color in Figure 3. Our simulation result is similar to the results in [23] and consistent with the experimentally observation [25]. The formation of secondary branches, their growth and competition, and finally their coarsening are obtained. The strong interaction between dendrites can be seen when the dendrites approach each other. The impingement between dendrites will hinder the growth of two dendrites. The high concentration was formed between the arms or in the domains where the impingement occur, because the solute is not easy to diffuse.

4.3 3D Numerical Experiment

We test the algorithm in a 3D cubic domain $[0, 1] \times [0, 1] \times [0, 1]$, using artificial data as follows: $L/c_p = 1$, $K/h = 1$, $T_L^{EQ} = 0.14$, $K/c_p = 1$, $C_0 = 0.1$, $m_L = -1$, $k = 0.8$, $D_S = D_L = 10^{-4}$ without consideration of curvature undercooling. The mesh is $256 \times 256 \times 256$ and the algorithm was implemented in parallel with MPI and the computation was carried on the PC cluster LSSC-II of the State Key Laboratory of Scientific and Engineering Computing. A $4 \times 4 \times 4$ computational nodes was adopted in our computation. The crystal profile obtained from the numerical result is in Figure 4.

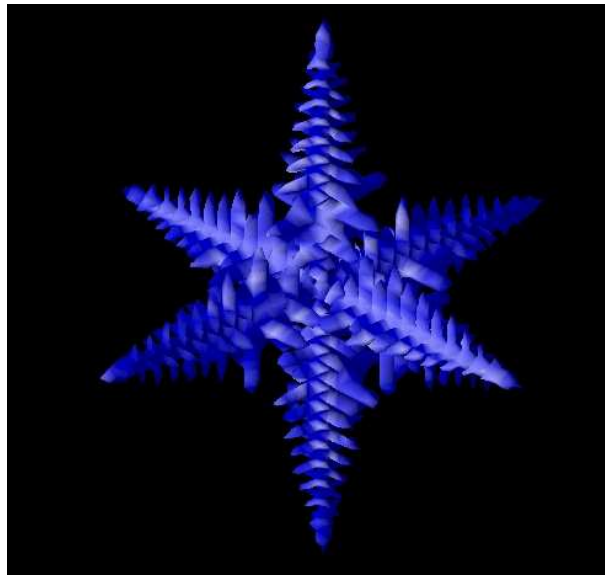


Figure 4: simulated 3D equiaxed crystal on $256 \times 256 \times 256$ mesh.

5 Conclusions

A new coupled model in binary alloy solidification, based on the cellular automaton technique has been developed. The temperature diffusion without the release of latent heat and solute diffusion are solved in the entire domain (at the macro-scale level). At the interface cells (at the micro-scale level), the energy and solute conservation, thermodynamic and chemical potential equilibrium are adopted to calculate the temperature, solid concentration, liquid concentration and the variation of solid fraction. The variation of solid fraction in this model is obtained by solving a four variables, quadratic algebraic system which has been checked that there is only one physical solution and it is very cheap to get the solution. Different from other models, the calculation of S/L interface velocity is not needed which means there are no any explicit or implicit cell resolution operations are required in the whole model. After the micro-scale adjustment, every interface cell satisfies the chemical potential and thermodynamic equilibrium. The model can be directly applied to multiple spatial dimensional case and it is trivial to extend this model to multiple component alloy system.

Acknowledgements

The authors thank Professor Dianzhong Li for illustrative discussions. This work was supported by the Special Funds for Major State Basic Research (G1999032804), the Integrated Simulation of Material Production Processing and Technological Organization Properties for New-aged Iron and Steel (No. 2001AA339030) and the Joint Applied Mathematics Research Institute between Peking University and Hong Kong Baptist University.

References

- [1] M. E. Glicksman, E. Winsa, R. C. Hahn, T. A. Lograsso, S. H. Tirmizi, and M. E. Selleck: Isothermal dendrite growth — a proposed microgravity experiment, *Metall. Trans.*, 1988, vol. 19(A), pp. 1945.
- [2] M. A. Chopra, M. E. Glicksman, and M. B. Singh: Dendritic solidification in binary alloys, *Metall. Trans.*, 1988, vol. 19(A), pp. 3087.
- [3] W. Kurz and D.J. Fisher: *Fundamentals of Solidification*, 3rd edn. Trans Tech Publications, Aedermannsdorf, Switzerland, 1989
- [4] W. Kurz, B. Giovanola and R. Trivedi: Theory of microstructural development during rapid solidification, *Metall. Trans. A*, 1987, vol. 18(A), pp. 823.
- [5] J. Lipton, M. E. Glicksman, and W. Kurz: Equiaxed solidification growth in alloys at small supercooling, *Metall. Trans.*, 1987, vol. 18(A), pp. 341.
- [6] J. Lipton, W. Kurz and R. Trivedi: Rapid dendrite growth in undercooled alloys, *Acta Met.*, 1987, vol. 35, pp. 957.
- [7] R. Trivedi and W. Kurz: Solidification microstructures: a conceptual approach, *Acta Metall. mater.*, 1994, vol. 42A, pp. 15.
- [8] A. A. Wheeler, W. J. Boettinger and G. B. McFadden: Phase-field model for isothermal phase transitions in binary alloys, *Phys. rev. A*, 1992, vol. 45, pp. 7424.
- [9] A. A. Wheeler, B. T. Murray and R. J. Schaefer: Computation of dendrites using a phase field model, *Physics D*, 1993, vol. 66, pp. 243.
- [10] S. L. Wang, R. F. Sekerka, A. A. Wheeler, B. T. Murray, S. R. Coriell R. J. Braun and G. B. McFadden: Thermodynamically-consistent phase-field models for solidification, *Physica D*, 1993, vol. 69, pp. 189.
- [11] J. A. Warren and W. J. Boettinger: Prediction of dendritic growth and microsegregation patterns in a binary alloy using the phase-field method, *Acta Met.* 1995, vol. 43, pp. 689.
- [12] S. G. Kim, W. T. Kim and T. Suzuki: Interfacial compositions of solid and liquid in a phase-field model with finite interface thickness for isothermal solidification in binary alloys, *Phys. rev. E*, 1998, vol. 58, pp. 3316.
- [13] S. G. Kim, W. T. Kim and T. Suzuki: Phase-field model for binary alloys, *Phys. rev. E*, 1999, vol. 60, pp. 7186.
- [14] W. Shyy, H. S. Udaykumar, M. M. Rao and R. W. Smith: *Computational Fluid Dynamics with Moving Boundaries*. Taylor and Francis, London, 1996.
- [15] H. S. Udaykumar and W. Shyy: Simulation of interfacial instabilities during solidification—1. conduction and capillarity effects, *Int. J. Heat Mass Transfer*, 1995, vol. 38(11), pp. 2057.
- [16] S. G. R. Brown and J. A. Spittle: Computer simulation of grain growth and macrostructure development during solidification, *Mater. Sci. Technol.*, 1989, vol. 5, pp. 362.

- [17] J. A. Spittle, and S. G. R. Brown: Computer simulation of the effects of alloy variables on the grain structures of castings, *Acta Met.*, 1989, vol. 37(7), pp.1803
- [18] S. G. R. Brown, T. Williams and J. A. Spittle: A cellular automaton model of the steady-state free growth of a non-isothermal dendrite, *Acta Met.*, 1994, vol. 42, pp. 2893.
- [19] R. Sasikumar and R. Sreenivasan: Two dimensional simulation of dendrite morphology, *Acta Met.*, 1994, vol. 42, pp. 2381.
- [20] U. Dilthey, V. Pavlik and T. Reichel: Numerical simulation of dendritic solidification with modified cellular automata, in *Mathematical Modelling of Weld Phenomena 3*, H. Cerjak and H. K. D. H. Bhadeshia, eds., The institute of Materials, London, 1997, pp. 85-105.
- [21] L. Nastac: Numerical modeling of solidification morphologies and segregation patterns in cast dendritic alloys, *Acta Met.*, 1999, vol. 47, pp. 4253.
- [22] A. Jacot and M. Rappaz: A pseudo-front tracking technique for the modelling of solidification microstructures in multi-component alloys, *Acta Materialia*, 2002, vol. 50, pp. 1909-1926.
- [23] L. Beltran-Sanchez and D. M. Stefanescu: Growth of solutal dendrites: a cellular automaton model and its quantitative capabilities, *Mat. and Mat. Trans. A*, 2003, vol. 26, pp. 367.
- [24] D. B. Kothe, R. C. Mjolsness, and M. D. Torrey: RIPPLE: A computer program for incompressible flows with free surface, LA-10612-MS, Los Alamos National Lab., Los Alamos, NM, 1991.
- [25] Weiming Feng, QingYan Xu and Baicheng Liu: Microstructure simulation of aluminum alloy using parallel computation technique, *ISIJ International*, 2002, Vol. 42, No. 7, pp.702.
- [26] J. Ni and C. Beckermann: A volume-averaged two-phase model for transport phenomena during solidification, *Metall. Trans*, 1991, Vol. 22B, pp. 349.

中文摘要

本文发展了一种模拟合金凝固过程中晶体生长的耦合模型。这个模型基于元胞自动机模型，能够模拟由温度场和浓度场以及其中的吉布斯-汤姆逊效应决定的晶体表面。我们在整个区域中求解不包含相变潜热的热扩散方程和溶质扩散方程。在界面胞中，根据能量守恒，溶质守恒，化学势平衡和热力学平衡，我们可以更新界面胞中的固相份数，从而得到满足化学势平衡和热力学平衡的固相和液相溶质浓度，并通过温度更新考虑到相变潜热释放。相比于文献中的一些模型使用某些计算界面速度的方法来更新固相份数，我们这个模型中的操作只需要解一个二阶的代数方程即可完成，完全不需要假设一个清晰的固液界面的存在，更不用计算这个界面的速度。这个模型可以自然的使用在任意的空间维数，略做简单推广，就能够计算任意多组份溶质合金的问题。本文的最后给出了数值实验的结果。